Extracellular Volume Fraction By Computed Tomography Predicts Long-Term Prognosis Among Patients With Cardiac Amyloidosis

Francisco Gama, MD [a,h,*], Stefania Rosmini, MD [a,*], Steve Bandula, PhD [b], Kush P Patel, MD MBBS [a,d], Paolo Massa, MD [i], Catalina Tobon-Gomez, PhD [c], Karolin Ecke [c], Tyler Stroud [c], Mark Condron [c], George D Thornton, MD MBBS [a,d], Jonathan B Bennett, MD [a,d], Ashutosh Wechelakar, PhD [f], Julian D Gillmore, PhD [f], Carol Whelan, MD [b,d,f], Helen Lachmann, PhD[f], Stuart Taylor, PhD [e], Francesca Pugliese, PhD [a,f], Marianna Fontana, PhD [b,d,f,], James C Moon, MD [a,d], Philip N Hawkins, PhD [f], Thomas A Treibel, PhD [a,d]

[*]Authors contributed equally
[a] Barts Heart Centre, St Bartholomew's Hospital, London, UK.
[b] UCL Centre for Medical Image Computing, Department of Medical Physics, London, UK.
[c] Canon Medical Systems Europe,
[d] Institute of Cardiovascular Science, University College London, London, UK.
[e] Centre for Medical Imaging, University College London, London, UK
[f] Queen Mary University of London.
[g] National Amyloidosis Centre, University College London, Royal Free Hospital, London, UK
[h] Hospital Santa Cruz, Centro Hospitalar Lisboa Ocidental, PT
[i] University Sant'Orsola Hospital, Bologna, Italy

Brief Title: ECV quantification by CT in amyloid patients

Manuscript Type: Original**; Manuscript:** 4880 words

Correspondence Address:
Dr Thomas Treibel PhD MBBS MRCP MA
Barts Heart Centre
St Bartholomew's Hospital
2nd Floor, King George V Block
London EC1A 7BE, United Kingdom
Tel: +44 20 346 56336 Fax: +44 2034563086
Email: Thomas.Treibel.12@ucl.ac.uk
Twitter: @ThomasTreibel

Tweet: Cardiac amyloid burden quantified by ECV_{CT} correlates with adverse remodeling and all-cause long-term mortality among ATTR patients. ECV_{CT} may address the need for better identification and risk stratification of amyloid patients, using a widely-accessible imaging modality. #JACC HF #CardioTweeter

Funding: JCM and TAT are directly and indirectly supported by the University College London Hospitals NIHR Biomedical Research Centre and Biomedical Research Unit at Barts Hospital, respectively. This work was undertaken at University College London Hospital, which received a proportion of funding from the UK Department of Health National Institute for Health Research Biomedical Research Centres funding scheme. KP is funded by the British Heart Foundation Clinical Research Training Fellowship. FG is supported by a non-restricted educational grant by Pfizer. TAT and MF are funded by British Heart Foundation intermediate fellowships (FS/19/35/34374 and FS/18/21/33447). GT is supported by BHF Clinical Research Training Fellowship (FS/CRTF/21/24128).

ABSTRACT (292/300 words)

Background: Light chain (AL) and transthyretin (ATTR) amyloid fibrils are deposited in the extracellular space of the myocardium, resulting in heart failure and premature mortality. Extracellular expansion can be quantified by CT, offering a rapid, cheaper and more practical alternative to cardiovascular magnetic resonance (CMR), especially among patients with cardiac devices or on renal dialysis.

Objectives: This study sought to investigate the association of extracellular volume fraction by computed tomography (ECV_{CT}), myocardial remodeling and mortality in patients with systemic amyloidosis.

Methods: Patients with confirmed systemic amyloidosis and varying degrees of cardiac involvement underwent ECG-gated cardiac CT. ECV_{CT} was analysed in the inter-ventricular septum. All patients also underwent clinical assessment, ECG, echocardiography, serum amyloid protein component (SAP) and/or technetium-99m (^{99m}Tc) 3,3-diphosphono-1,2-propanodicarboxylic acid scintigraphy. ECV_{CT} was compared across different extents of cardiac infiltration (ATTR Perugini Grade / AL Mayo Class) and evaluated for its association with myocardial remodeling and all-cause mortality.

Results: 72 patients were studied (AL n= 35, ATTR n= 37; age 67 (59-76) years, 71% males). Mean septal ECV_{CT} was 42.7±13.1% and 55.8±10.9% in AL and ATTR, respectively, and correlated with indexed left ventricular (LV) mass (r=0.426, p<0.001), LV ejection fraction [LVEF, (r=0.460, p<0.001)], NT-proBNP (r=0.563, p<0.001) and hsTnT (r=0.546, p=0.02). ECV_{CT} increased with cardiac amyloid involvement in both AL and ATTR. Over a mean follow-up of 5.3 ± 2.4 years, 40 deaths occurred (AL 14 [35%]; ATTR 26 [65%]). ECV_{CT} was independently associated with all-cause mortality in ATTR (not AL) after adjustment for age and IV septal wall thickness (HR:1.046, 95%CI:1.003-1.090, p=0.037).

Conclusion: Cardiac amyloid burden quantified by ECV_{CT} is associated with adverse cardiac remodeling as well as all-cause mortality among ATTR amyloid patients. ECV_{CT} may address the need for better identification and risk stratification of amyloid patients, using a widely-accessible imaging modality.

KEYWORDS: Computed tomography; Myocardial tissue characterization; Extracellular matrix; Myocardial extracellular volume fraction; Myocardial fibrosis; cardiac amyloidosis.

LIST OF ABBREVIATIONS

AL amyloidosis = Immunoglobulin light-chain amyloidosis

ATTR = Aortic stenosis

CT = Computed tomography

CMR = Cardiovascular magnetic resonance

ECV = Extracellular volume fraction

GLS = Global longitudinal strain

hsTnT = high-sensitivity troponin T

HFpEF = Heart Failure with preserved ejection fraction

HU = Hounsfield units

LV = Left ventricle

WT = wild type

INTRODUCTION

Systemic amyloidosis is a multisystem disease caused by the deposition of misfolded fibrillar protein into tissues causing expansion of the extracellular space and impairment of function [1,2]. Myocardial infiltration by light chain (AL) or transthyretin (ATTR) amyloid fibrils causes heart failure and is associated with poor prognosis [3-5]. Over the last two decades, advances in multi-modality assessment, incorporating echocardiography with strain, contrast enhanced cardiovascular magnetic resonance (CMR) and bone scintigraphy have highlighted that cardiac amyloidosis has a much higher prevalence than previously thought. In particular ATTR amyloidosis has been found in multiple settings of heart failure, for example in 13% of patients with heart failure with preserved ejection fraction (HFpEF) [6] and 1 in 7 elderly patients (aged 75 years and over) with severe aortic stenosis (AS) undergoing transcatheter aortic valve intervention [7-9]. The advent of multiple novel therapeutic options [10-12] brings to the fore the pressing need for early identification of cardiac amyloidosis. Myocardial infiltration by amyloid fibrils causes extracellular expansion and this can not only be diagnosed, but also quantified by ECV imaging using CMR [13,14] and CT [15-19]. ECV quantification by CT (ECV_{CT}), although less established, offers key advantages over CMR as it is easily added to routine CT coronary angiography by the simple addition of a post-contrast phase [15-19], especially in patients already undergoing CT for other indications. ECV_{CT} is fast (3 minutes extra) and well-tolerated by patients and is therefore an economical alternative to CMR and scintigraphy which are less widely available. Furthermore, ECV_{CT} can be used in patients with cardiac pacemakers or defibrillators or patient undergoing cardiac CT for other indications (e.g. work-up for transcatheter aortic valve replacement).

We sought to investigate the feasibility of quantifying ECV_{CT} to assess its association with cardiac remodeling and mortality in patients with systemic amyloidosis.

MATERIAL AND METHODS

All research was carried out at University College London Hospital and the Royal Free NHS Trusts, London, UK, between January 2013 and February 2016. The study was approved by the ethical committee of the U.K. National Research Ethics Service (REC reference 09/H0716/75) and conformed to the principles of the Helsinki Declaration. All subjects gave written informed consent to participate in the study. Exclusion criteria were uncontrolled arrhythmia, significant valve disease and impaired renal function (estimated glomerular filtration rate <45mL/min). ATTR sub-cohort patients were not under any disease modifying therapy (not available in the UK or were either enrolled into dedicated trials at the time).

All patients underwent 12-lead ECG, echocardiography, assays of N-terminal pro-brain natriuretic peptide (NT-proBNP), high-sensitivity troponin T (hsTnT) and 6-minute walk test (6MWT) where health and patient choice permitted (e.g. arthritis, postural hypotension, neuropathy). Prior to the scan, following insertion of an intravenous cannula, a 2-mL blood sample was collected and sent for complete blood cell count analysis; hsTnT and NT-proBNP were measured clinically. Transthoracic echocardiography (TTE) was performed for assessment of left ventricular (LV) structure [i.e LV mass, interventricular (IV) septal thickness, atrial volume, valvular disease], systolic and diastolic function, and global longitudinal strain (GLS) according to the European Society of Echocardiography criteria[20]. Concomitant cardiac CMR at the time of enrollment was limited by local availability, patient agreement and tolerance.

ATTR patients underwent bone scintigraphy using 3,3-diphosphono-1,2-propanodicarboxylicacid (DPD)[21], whereas AL patients also underwent SAP scintigraphy. For ATTR, cardiac amyloidosis was defined by presence of ATTR amyloid in a myocardial biopsy (Congo red and immunohistochemical staining) or positive DPD scintigraphy. DPD scans were reported by two experienced clinicians using the Perugini grading system[21], where Grade 0

represents no cardiac uptake with normal bone uptake (i.e. negative) and Grades 1-3 represent increasing cardiac uptake with increasing bone attenuation. All ATTR patients also underwent sequencing of exons 2, 3, and 4 of the TTR gene.

For AL, systemic AL amyloidosis was proven with biopsies from non-cardiac tissues. Light chain cardiac deposition was assessed according to Mayo staging system that grades heart involvement considering the expected cardiotoxic effect (assessed by cardiac troponin and NTproBNP levels) in addition to the difference between involved and uninvolved serum free light chains [22-24].

Twenty-seven patients with severe aortic stenosis (AS) (68±8 years, 19 male) were included as a comparator cohort. Cardiac amyloidosis was excluded by myocardial biopsy (Congo red staining) taken during aortic valve surgery[18].

ECV_{CT} Protocol.

The CT protocol consisted of three steps: first, a low dose non-contrast scan to obtain baseline attenuations; second, contrast administration with a contrast-enhanced 30 seconds acquisition; third, a 5 minute delay to allow blood to myocardial contrast equilibration followed by a repeat scan to re-measure blood and myocardial attenuations. CT examinations were performed either on a 320–detector row CT scanner (Aquilion ONE Vision™; Canon Medical Systems Corp., Tokyo, Japan) or a 64-detector row CT scanner (Somatom Sensation 64; Siemens Medical Solutions, Erlangen, Germany). A topogram was used to plan CT volumes from the level of the aortic valve to the inferior aspect of the heart, typically a 10 cm slab. Cardiac scans (tube voltage, 120 kV; tube current–time product, 160 mAs; section collimation, 320 or 64 detector rows, 1.2-mm section thickness; gantry rotation time, 275 msec [320-detector] / 330ms [64-detector]) were acquired with prospective gating (65%–75% of R-R interval) and reconstructed into axial sections. All pre- and post-contrast acquisitions were performed and reconstructed

with the same parameters and matched the level of the pre-contrast scan. The iodinated contrast material used was iohexol (Omnipaque 300; Nycomed Amersham, Oslo, Norway; 300 mg of iodine per milliliter) at a standard dose of 1mL/kg and injection rate of 3ml/sec without a saline chaser. Radiation exposure was quantified using the dose-length product multiplied by a chest conversion coefficient (κ=0.028mSv/mGy.cm)[25].

Image Analysis.

Septal analysis. All three acquired phases (baseline, angiography, post-contrast) were co-registered using a non-rigid co-registration algorithm, and then segmented using an in-house cardiac atlas algorithm. Pixel-by-pixel myocardial ECV was then calculated from the segmented left ventricular myocardial and blood attenuation values (pre-and post-contrast only) from the ratio of the change in blood and myocardial attenuation (ΔHU) corrected by the blood volume of distribution (1 – Hematocrit); the hematocrit was manually inputted using study visit laboratory result: $ECV = (1 - \text{Hematocrit}) \times (\Delta HU_{tissue} / \Delta HU_{blood})$

Whole heart analysis. Whole heart CT image visualization was performed using a custom-designed registration and segmentation software (this was not performed in the Siemens cohort as the earlier protocol did not cover the whole heart). The resulting ECV volume was superimposed over the co-registered angiographic phase for visualization and outputted in an AHA segment format. In patients with history or evidence of myocardial infarction on imaging, affected segments were excluded from analysis.

Statistical analysis

Analysis was performed according to amyloid subtype (i.e AL and ATTR) considering the differences in natural history, age and non-cardiac organ involvement. Continuous variables are described as mean ± SD or as median [interquartile range], while categorical variables are

described as percentages. Normal distribution was assessed by using the Shapiro-Wilk test. To compare variables, Student's t-test or Mann Whitney were used for continuous variables, as appropriate and chi-square test for categorical variables. Correlation between ECV and clinical parameters were performed with Pearson' or Spearman analysis accordingly. Univariable and multivariable (backward stepwise selection approach) Cox proportional hazards models were used to examine the prognostic importance of a broad range of baseline parameters to all-cause death. Clinically relevant variables that demonstrated statistical significance in univariable analysis (P value ≤ 0.05) were selected for the multivariable analysis. Event-free survival curves associated with ECV_{CT} were examined using the Kaplan-Meier method and compared with the log-rank test. All tests were 2-sided and a p-value<0.05 was considered as statistically significant. SPSS statistics software version 25.0 (SPSS, Chicago, Illinois) was used to perform all statistical evaluations.

RESULTS

Study population

72 patients with a confirmed diagnosis of either AL (n=35) or ATTR (n=37) amyloid were included is this study. Median age was 67 (59-76) years, 51 (70.8%) males. Among the 37 ATTR cases, 21 had wtATTR and 16 had hereditary ATTR with identified genetic mutations (supplementary table 1). All ATTR patients had cardiac involvement, 4 (10.8%) had Perugini grade 1, 26 (70.3%) grade 2 and the remaining (18.9%) grade 3. In the AL cohort, 5 patients had no cardiac involvement, while n=10 were in Mayo class1, n=15 in Mayo 2 and n=5 in Mayo class 3. Compared to patients with AL amyloidosis, those with ATTR subtype were predominantly males (n=35, 94.6% vs n=16, 45.7%, p<0.001), older [74 (63-78) vs 62 (56-70], p=0.005), and with more hypertrophy [LV mass indexed: 154 (120-179) g/m^2 vs 96 (82-140) g/m^2, p=0.01; IV septal thickness:15.8±3.6mm vs 13.4±3.1mm, p=0.005], see Table 1.

ECV analysis

Mean septal ECV for the study population was 49±14%. Patients with ATTR amyloid had significantly higher septal ECV percentages compared to AL subtype (56±11% vs 43±13%, p<0.001). This variable significantly correlated with indexed LV mass (r=0.426, p<0.001), left ventricular ejection fraction [LVEF, (r=0.460, p<0.001)] and biomarkers of myocardial injury [NT-proBNP (r=0.563, p<0.001) and hsTnT (r=0.546, p=0.02)]. GLS failed to correlate with ECV (r=0.18, p=0.043) and with prognosis among ATTR (HR:0.902, 95%CI:0.810-1.005, p=0.062) and AL (HR:0.990, 95%CI:0.878-1.116, p=0.871) population. ECV percentages correlated both with increased cardiac involvement in AL (Mayo Class; p=0.003) and ATTR amyloid (Perugini Grade; p=0.002). Significant differences were observed between Mayo grade 0/1 and 2/3 (35±10% vs 49±13%, p =0.003) in AL and between Perugini grade 1 and 2/3 (36±8% vs 58±9%, p<0.001) in ATTR, see figure 1.

Thirty-nine patients (54.1%) underwent whole heart ECV analysis, whose global quantification yielded a satisfactory correlation with septal ECV (r=0.72; p=0.002). ECV polar maps visually represented absence of amyloid infiltration vs early infiltration vs severe infiltration (see figure 2). Furthermore, ECV polar maps were still diagnostic in patients with pacemakers and defibrillators and had the ability to identify regional elevated ECV due to myocardial infarction (see figure 3).

Patients with amyloid disease had significantly higher ECV than AS patients waiting for AVR (49.4 ± 13.7 vs 28.3 ± 4.6%, p<0.001, see figure 4A).

Outcome

Over a mean follow-up of 5.3 ± 2.4 years, 40 out of 72 patients died (n=26 out of 37 ATTR; 14 out of 35 AL). Deceased patients were older [74 (62-78) vs 62 (57-69), p=0.014), with higher

NT-proBNP levels [199 (141-401) pg/mL vs 49 (17-149) pg/mL, p<0.001]. These patients had more LV hypertrophy [LV mass indexed: 148 (116-174) g/m^2 vs 105.5 (71-145.3) g/m^2, p=0.009 and septal wall thickness: 15.6±3.1mm vs 13.2±3.6mm, p=0.006] with higher severity of diastolic dysfunction [Deceleration time: (182 (154.0–212.0) ms vs 215.0 (174.0–248.0) ms, p=0.036 and E/e' average=[16.0 (13.8–19.3) vs 11.1 (8.3–14.4), p-value=0.018], see Supplemental Table 2.

In the ATTR population, more than two thirds of patients died (n=26, 70.3%) at a mean follow up of 5.1±2.4 years. Patients who died were older [77 (67-79) vs 65 (56-71) years, p=0.016], had higher cardiac biomarkers [NT-proBNP (p=0.009) and hsTnT (p=0.002)], increased LV myocardial mass [LV mass indexed: 160 (144-180) vs 122 (68-179)g/m^2, p=0.028; IV septal thickness: 16.6±3.3 vs 13.6±3.5 mm, p=0.027], worse LVEF (47±12% vs 58±19%, p=0.043) and higher septal ECV_{CT} (58±8% vs 50±14%, p=0.036) (Table 2). These variables remained significant predictors of all-cause death on univariate Cox regression analysis (Table 3). Septal ECV_{CT} was independently associated with mortality among ATTR patients in multivariate Cox regression analysis adjusted for age, IV septal wall thickness and LVEF [hazards ratio (HR):1.047, 95% confidence interval (CI):1.005-1.091, p=0.027]. Global ECV_{CT} failed to do so on univariate analysis [HR:1.037, 95%CI:0.942-1.141, p=0.451]

In the AL population, fourteen patients (40%) died over a mean follow-up of 5.5 ± 2.4 years, without any difference regarding baseline chemotherapeutic regime. At baseline, patients who died had significantly higher levels of NTproBNP [152 (89-429) pg/mL vs 67 (15-146) pg/mL, p=0.004] and average global ECV (39 ± 9 % vs 48 ± 9 %, p=0.021) percentages (supplemental table 3). In addition, this later variable was a significant predictor of all-cause mortality on cox regression univariate analysis (HR: 1.090, 95%CI:1.016-1.169, p=0.016), contrasting with septal ECV (HR: 0.989, 95%CI:0.941-1.040, p=0.667.

Forty-one patients (57%) underwent cardiac CMR at the time of enrollment. Extracellular volume by CT significantly correlated with that acquired by CMR (r=0.8; p<0.001; see figure 4B). This variable failed to predict the outcome among AL population (p=0.545). However, CMR_{ECV} significantly predicted the outcome of patients with ATTR subtype (HR: 1.018, 95%CI:1.001-1.082, p=0.042), yielding a similar ROC curve as ECV by CT [c-index=0.68, 95%CI: 0.469-0.884 vs c-index=0.72, 95%CI:0.456-0.988; p=0.957).

DISCUSSION

In our cohort of patients with both AL and ATTR amyloidosis and varying degree of cardiac involvement, we found that septal ECV by cardiac CT obtained as a marker of amyloid cardiac burden was associated with LV hypertrophy and function, level of cardiac involvement as well as NT-proBNP and hsTnT. Furthermore, among patients with ATTR amyloidosis, ECV_{CT} was independently associated with all-cause mortality. As such, ECV_{CT} replicates previous findings of ECV by CMR, namely as a marker of amyloid burden and outcome in ATTR. Greater availability of ECV_{CT} and ease for patients compared to CMR (3 versus 45 min protocol) suggests that this technique could be considered as an alternative modality for diagnosis, monitoring and risk stratification.

Considering the different pathophysiology, clinical manifestations, treatment options and prognosis in AL and ATTR, we have conducted the outcome analysis separately. In ATTR cohort, patients were older, had higher LV mass, increased myocardial injury biomarkers and increased ECV_{CT}; and these parameters were independently associated with all-cause mortality. Consistent with previous CMR studies showing the prognostic value of ECV in ATTR, ECV_{CT} remained an independent predictor of mortality in this cohort, confirming its added value for risk stratification[26,27]. As for the AL sub-cohort, only whole heart ECV had prognostic value, raising the possibility of different amyloid distributions depending on the pathology. Further

studies with an increased number of patients are needed to confirm this association. Furthermore, survival in our AL cohort was better than in ATTR and longer than expected by current literature [28-30]. In addition to a relatively small cohort, we were also limited by our initial ethics committee mandating a relatively high cut-off for exclusion (eGFR>45mL/min/m^2) whereas it is lower in clinical practice. This may have resulted in recruitment of patients with significantly less multisystemic organ failure and consequently better outcome. Moreover, not every patient within the AL arm had cardiac involvement exemplified by a significantly lower myocardial ECV (whereas all ATTR patients had cardiac involvement). Finally, the fact that AL prognosis is influenced by the variable response to chemotherapy contrasting with the fact that ATTR patients did not undergo any disease modifying therapy might have additionally influenced the outcome of this cohort. Recent data by the UK National Amyloidosis Centre shows that ECV guides monitoring of cardiac involvement in AL, and the role of ECV_{CT} in AL monitoring and prognostication will require larger cohort investigation[31].

Increased cardiac afterload by severe AS is a biomechanical stressor responsible for enhanced proinflammatory and collagen turnover signaling that causes interstitial remodeling through synthesis and deposition of ECV[32]. This group already showed that ECV can be readily accessible by cardiac CT, with a good correlation with CMR[33]. In this study, we ascertain this finding, and additionally confirm the utility of cardiac CT in differentiating two different pathologies responsible for distinct forms of interstitium remodeling.

Wider access to diagnostic modality for the identification of interstitial heart disease is important[34] – ECV quantification by CT, despite its lower signal to noise ratio, has key advantages over CMR: The CT approach is cheaper (for example the UK tariff for cardiac CT is less than a third of the CMR tariff, whereas in the US is less than half) and widely available, can now be completed in 3 minutes[35], and the scanner design can accommodate patients with obesity and claustrophobia (while CMR is not suitable in around 10% of patients due to

claustrophobia or is at risk in patients with CMR non-compatible cardiac devices)[36]. Finally, the concentration of iodine has a linear relationship with the CT attenuation value, which is not affected by fast exchange mechanism like CMR T1 mapping (depending on cell size and contrast dose, fast transcytolemmal water-exchange may reach its limits), which do not apply to CT [37, 38].

ECV (by CMR or CT) allows quantification of a key pathophysiological pathway in heart failure: interstitial expansion due to diffuse myocardial fibrosis (or in rare cases by deposition of amyloid fibrils)[15-18]. As the CMR field is showing, ECV is diagnostic in certain diseases, tracks myocardial remodeling and predicts outcome [39,40]. In this study, ECV by CT significantly correlated with CMR with similar prognosis ability, although limited sample comparison hinders strong conclusions in this regard. Due to the aforementioned advantages of CT over CMR, ECV by CT will undoubtedly receive greater attention as part of comprehensive assessment of the heart by CT coronary angiography, perfusion and myocardial tissue characterization. Furthermore, with the general epidemiologic trend of increasing prevalence of wt-ATTR and the recent development of new targeted drugs for the treatment of amyloid deposition[41], an early diagnosis of this condition is of key importance and cardiac CT could represent a contributing diagnostic method.

Moreover, the use of 3D isotropic visualisation and quantification of ECV by cardiac CT allows the identification of different patterns of scar and infiltration, not only as a per segment distribution (i.e subendocardial, epicardial or mid-wall), but also for the extension of the fibrosis/amyloid burden throughout the left ventricle assessed by the AHA segmentation. Also, as shown in the Figure 3C, ECV interpretability is preserved even in the presence of artefacts like those caused by pacemaker/ICD leads whose beam hardening should not disrupt assessment of neighboring segments. Conversely, the magnetic field change expected to occur due to device interference, can generate non-diagnostic and possibly mis-leading T1 and ECV

assessment, hindering tissue evaluation with CMR in this subset[42]. Previous studies already showed a strong correlation with affected myocardial infarct area and matching culprit coronary artery disease assessed CT coronary angiogram[43]. Although broader validation studies of this technique are still required, these are important advantages offering an interesting alternative to CMR, currently the most used modality for myocardial tissue characterisation.

This study has limitations. The study cohort is limited in size which restricts ability to make wider mechanistic associations. As patients were recruited from a national referral center, a referral bias may have affected the results. The effect of treatment in patients with AL amyloidosis has been acknowledged and discussed above. Furthermore, even though all included patients had septal ECV analysis, only half had simultaneous global ECV by CT and/or ECV by CMR, restricting comparison between acquisitions. The only outcome variable provided was all-cause mortality, hindering the ability to establish strong correlations between baseline variables and other relevant cardiovascular events (i.e hospitalizations, cardiovascular mortality).

CONCLUSION

In patients with AL or ATTR amyloidosis, ECV by cardiac CT correlates with parameters of adverse myocardial remodeling and is independently associated with all-cause mortality in ATTR subtype. ECV_{CT} replicates previous findings of ECV by CMR but the fastest acquisition, cheaper and widespread accessibility of this imaging modality are deemed as important advantages. ECV_{CT} may address the need for better identification and risk stratification of amyloid patients.

PERSPECTIVES

COMPETENCIES IN MEDICAL KNOWLEDGE

Cardiac amyloidosis is a disorder caused by extracellular deposition of amyloid fibrils in the myocardium resulting in heart failure and premature mortality. Heightened clinicians' awareness and increased use of cardiac MRI has increased the diagnosis of cardiac amyloidosis. Cardiac CT offers an appealing alternative, and is quicker, cheaper, less claustrophobic and less affected by cardiac devices. In this study, amyloidosis quantification using ECV by CT correlated well with cardiac injury biomarkers, hypertrophy, worse ejection fraction, cardiac involvement, and increased mortality during long-term follow-up among patients with amyloidosis.

TRANSLATIONAL OUTLOOK

Extracellular volume fraction (ECV) detected by cardiac CT has the potential to improve recognition of cardiac amyloidosis. ECV_{CT} replicates previous findings of CMR but is faster to acquire, less claustrophobic and has widespread availability and is significantly cheaper. ECV_{CT} may address the need for better identification and risk stratification of amyloid patients, using a widely available imaging modality. This becomes even more important considering the negative burden of this pathology and the fact that there are promising new pharmacological therapies that improve patients' prognosis.

REFERENCES

1. Banypersad SM, Moon JC, Whelan C, Hawkins PN, Wechalekar AD. Updates in cardiac amyloidosis: a review. J Am Heart Assoc 2012;1(2):e000364.

2. Merlini G, Bellotti V. Molecular mechanisms of amyloidosis. N Engl J Med 2003;349(6):583-96.

3. Ng B, Connors LH, Davidoff R, Skinner M, Falk RH. Senile systemic amyloidosis presenting with heart failure: a comparison with light chain-associated amyloidosis. Arch Intern Med 2005;165(12):1425-9.

4. Dubrey SW, Cha K, Skinner M, LaValley M, Falk RH. Familial and primary (AL) cardiac amyloidosis: echocardiographically similar diseases with distinctly different clinical outcomes. Heart 1997;78(1):74-82.

5. Rapezzi C, Merlini G, Quarta CC, et al. Systemic cardiac amyloidoses: disease profiles and clinical courses of the 3 main types. Circulation 2009;120(13):1203-12.

6. Gonzalez-Lopez E, Gallego-Delgado M, Guzzo-Merello G, et al. Wild-type transthyretin amyloidosis as a cause of heart failure with preserved ejection fraction. Eur Heart J 2015;36(38):2585-94.

7. Scully PR, Treibel TA, Fontana M, et al. Prevalence of Cardiac Amyloidosis in Patients Referred for Transcatheter Aortic Valve Replacement. J Am Coll Cardiol 2018;71(4):463-464.

8. Castano A, Narotsky DL, Hamid N, et al. Unveiling transthyretin cardiac amyloidosis and its predictors among elderly patients with severe aortic stenosis undergoing transcatheter aortic valve replacement. Eur Heart J 2017;38(38):2879-2887.

9. Cavalcante JL, Rijal S, Abdelkarim I, et al. Cardiac amyloidosis is prevalent in older patients with aortic stenosis and carries worse prognosis. J Cardiovasc Magn Reson 2017;19(1):98.

10. Maurer MS, Schwartz JH, Gundapaneni B, et al. Tafamidis Treatment for Patients with Transthyretin Amyloid Cardiomyopathy. N Engl J Med 2018.

11. Adams D, Gonzalez-Duarte A, O'Riordan WD, et al. Patisiran, an RNAi Therapeutic, for Hereditary Transthyretin Amyloidosis. N Engl J Med 2018;379(1):11-21.

12. Benson MD, Waddington-Cruz M, Berk JL, et al. Inotersen Treatment for Patients with Hereditary Transthyretin Amyloidosis. N Engl J Med 2018;379(1):22-31.

13. Ugander M, Oki AJ, Hsu LY, et al. Extracellular volume imaging by magnetic resonance imaging provides insights into overt and sub-clinical myocardial pathology. Eur Heart J 2012;33(10):1268-78.

14. Banypersad SM, Fontana M, Maestrini V, et al. T1 mapping and survival in systemic light-chain amyloidosis. Eur Heart J 2015;36(4):244-51.

15. Bandula S, White SK, Flett AS, et al. Measurement of myocardial extracellular volume fraction by using equilibrium contrast-enhanced CT: validation against histologic findings. Radiology 2013;269(2):396-403.

16. Nacif MS, Kawel N, Lee JJ, et al. Interstitial myocardial fibrosis assessed as extracellular volume fraction with low-radiation-dose cardiac CT. Radiology 2012;264(3):876-83.

17. Nacif MS, Liu Y, Yao J, et al. 3D left ventricular extracellular volume fraction by low-radiation dose cardiac CT: assessment of interstitial myocardial fibrosis. J Cardiovasc Comput Tomogr 2013;7(1):51-7.

18. Treibel TA, Bandula S, Fontana M, et al. Extracellular volume quantification by dynamic equilibrium cardiac computed tomography in cardiac amyloidosis. J Cardiovasc Comput Tomogr 2015.

19. Kurita Y, Kitagawa K, Kurobe Y, et al. Estimation of myocardial extracellular volume fraction with cardiac CT in subjects without clinical coronary artery disease: A feasibility study. J Cardiovasc Comput Tomogr 2016;10(3):237-41.

20. Marizio G, Cosyns B, Edvardsen T, et al. Standardization of Adult Transthoracic Echocardiography Reporting in Agreement with Recent Chamber Quantification, Diastolic

Function, and Heart Valve Disease Recommendations: An Expert Consensus Document of the European Association of Cardiovascular Imaging. *European Heart Journal - Cardiovascular Imaging* 18, no. 12 (1 December 2017): 1301–10.

21. Perugini E, Guidalotti PL, Salvi F, et al. Noninvasive etiologic diagnosis of cardiac amyloidosis using 99mTc-3,3-diphosphono-1,2-propanodicarboxylic acid scintigraphy. J Am Coll Cardiol 2005;46(6):1076-84.

22. Gertz MA, Comenzo R, Falk RH, et al. Definition of organ involvement and treatment response in immunoglobulin light chain amyloidosis (AL): a consensus opinion from the 10th International Symposium on Amyloid and Amyloidosis, Tours, France, 18-22 April 2004. Am J Hematol 2005;79(4):319-28.

23. Fontana M, Banypersad SM, Treibel TA, et al. Native T1 mapping in transthyretin amyloidosis. JACC Cardiovasc Imaging 2014;7(2):157-65.

24. Shaji K, Dispenzieri A, Lacy MQ, et al. Revised Prognostic Staging System for Light Chain Amyloidosis Incorporating Cardiac Biomarkers and Serum Free Light Chain Measurements. *Journal of Clinical Oncology* 30, no. 9 (20 March 2012): 989–95.

25. Hausleiter J, Meyer T, Hermann F, et al. Estimated radiation dose associated with cardiac CT angiography. Jama 2009;301(5):500-7.

26. Martinez-Naharro A, Treibel TA, Abdel-Gadir A, et al. 2017. Magnetic Resonance in Transthyretin Cardiac Amyloidosis. *Journal of the American College of Cardiology* 70 (4): 466–77.

27. Martinez-Naharro A, Kotecha T, Norrington K, et al. Native T1 and Extracellular Volume in Transthyretin Amyloidosis. *JACC: Cardiovascular Imaging* 12, no. 5 (May 2019): 810–19.

28. Kyle RA, Linos A, Beard CM, et al. Incidence and Natural History of Primary Systemic Amyloidosis in Olmsted County, Minnesota, 1950 through 1989. *Blood* 79 (7): 1817–22.

29. Madan S, Shaji K.K, Angela D, et al. High-Dose Melphalan and Peripheral Blood Stem Cell Transplantation for Light-Chain Amyloidosis with Cardiac Involvement. *Blood* 119 (5): 1117–22.

30. Giampaolo M, Bellotti V. 2003. Molecular Mechanisms of Amyloidosis. *The New England Journal of Medicine* 349 (6): 583–96.

31. Martinez-Naharro A, Abdel-Gadir A, Treibel TA, et al. CMR-Verified Regression of Cardiac AL Amyloid After Chemotherapy. *JACC: Cardiovascular Imaging* 11, no. 1 (January 2018): 152–54.

32. Díez, Javier, Arantxa González, and Jason C. Kovacic. 'Myocardial Interstitial Fibrosis in Nonischemic Heart Disease, Part 3/4'. *Journal of the American College of Cardiology* 75, no. 17 (May 2020): 2204–18.

33. Treibel TA, Bandula S, Fontana M et al. Extracellular volume quantification by dynamic equilibrium cardiac computed tomography in cardiac amyloidosis. J Cardiovasc Comput Tomogr. 2015 Nov-Dec;9(6):585-92.

34. Schelbert EB, Fonarow GC, Bonow RO, Butler J, Gheorghiade M. Therapeutic targets in heart failure: refocusing on the myocardial interstitium. J Am Coll Cardiol 2014;63(21):2188-98.

35. Scully PR, Kush PP, Bunny S, et al. Identifying Cardiac Amyloid in Aortic Stenosis. *JACC: Cardiovascular Imaging* 13, no. 10 (October 2020): 2177–89.

36. Rosmini S, Treibel TA, Bandula S, et al. Cardiac computed tomography for the detection of cardiac amyloidosis. J Cardiovasc Comput Tomogr 2016.

37. Moon JC, Messroghli DR, Kellman P, et al. Myocardial T1 mapping and extracellular volume quantification: a Society for Cardiovascular Magnetic Resonance (SCMR) and CMR Working Group of the European Society of Cardiology consensus statement. J Cardiovasc Magn Reson 2013;15(1):92.

38. Coelho-Filho OR, Holland DJ, Mongeon FP, et al. Role of Transcytolemmal Water-Exchange in Magnetic Resonance Measurements of Diffuse Myocardial Fibrosis in Hypertensive Heart Disease. Circulation Cardiovascular imaging 2013;6(1):134-141.

39. Banypersad SM, Sado DM, Flett AS, et al. Quantification of Myocardial Extracellular Volume Fraction in Systemic AL Amyloidosis: An Equilibrium Contrast Cardiovascular Magnetic Resonance Study. Circulation Cardiovascular imaging 2013;6(1):34-39.

40. Wong TC, Piehler KM, Kang IA, et al. Myocardial extracellular volume fraction quantified by cardiovascular magnetic resonance is increased in diabetes and associated with mortality and incident heart failure admission. European Heart Journal 2013.

41. Griffin, JM, Rosenthal JL, Grodin JL, et al. ATTR Amyloidosis: Current and Emerging Management Strategies. *JACC: CardioOncology* 3, no. 4 (October 2021): 488–505

42. Bhuva AN, Treibel TA, Seraphim A, Scully P, Knott KD, Augusto JB et al. Measurement of T1 Mapping in Patients With Cardiac Devices: Off-Resonance Error Extends Beyond Visual Artifact but Can Be Quantified and Corrected. Front Cardiovasc Med. 2021 Jan 29;8:631366.

43. Palmisano A, Vignale D, Tadic M, et al. Myocardial Late Contrast Enhancement CT in Troponin-Positive Acute Chest Pain Syndrome. *Radiology*, 7 December 2021, 211288.

Tables

Table 1: Baseline population characteristic according to amyloid subtype.

	Total (N=72)	AL (N=35)	ATTR (N=37)	p-value
Demographics				
Male (%)	51(70.8)	16(45.7)	35(94.6)	<0.001
Age, years	67(59-76)	62(56-70)	74(63-78)	0.005
BSA, m^2	1.91±0.22	1.89±0.23	1.92±0.20	0.619
ECG				
Sinus rhythm, n (%)	65(90.3)	33 (94.3)	32(86.5%)	0.524
Atrial fibrillation, n (%)	3(4.2)	1(2.9)	2(5.4)	
Systolic arterial pressure, mmHg	134±8	130±12	136±7	0.678
Laboratory				
Hematocrit, %	40.5±4.4	39.2±4.6	41.7±3.8	0.013
eGFR, ml/min/m^2	73.8±14.2	77.2±13.8	70.6±14.0	0.046
NTproBNP, pg/mL	151(52-354)	104(29-309)	196(80–359)	0.174
hsTnT, ng/mL	0.044(0.019-0.065)	0.027(0.010-0.044)	0.051(0.028-0.073)	0.302
6MWT, m	355±147	383±155	331±138	0.153
Imaging assessment				
Septal ECV, %	49±14	43±13	56±11	<0.001
Global ECV, %	46±9	42±10	51±7	0.006
LV mass, g	253(168-311)	189(150-285)	294(229-371)	0.003
LV mass indexed, g/m^2	128(90-172)	96(82-140)	154 (120-179)	0.01
Max IVS thickness, mm	14.5±3.5	13.4±3.1	15.8±3.6	0.005
LVEF, %	56±15	62±12	50±15	<0.001
LAA, cm^2	23.7(19–30)	21.2(16.1-24.3)	27.8(22.5–33.1)	<0.001
RAA, cm^2	20.4(16.2–25.1)	16.9(13.0–20.5)	23.5(19.5–29.3)	<0.001
TAPSE, cm	1.8(1.4-2.4)	2.0(1.5–2.6)	1.5(1.2-2.3)	0.693
Dec Time, ms	194(158.5-229.5)	213(156.3–256.3)	187(165–209.3)	0.137
E/e' average	14 (10.6–18.4)	13.9(9.1–17.7)	14.3(12.4–19.2)	0.246
GLS, %	-14.8±5.7	-15.2±5.6	-14.7±5.8	0.760

BSA stands for body surface area, eGFR for estimated glomerular filtration rate, ECV for extracellular volume, hsTnT for high sensitive troponin T, Max IVS for maximum interventricular septum, LVEF for left ventricular ejection fraction, LAA for left atrium area, RAA for right atrium area, TAPSE for tricuspid annular systolic excursion, Dec for deceleration, and 6MWT for 6 minutes walking test.

Table 2: ATTR amyloidosis patients, according to survival status.

	Total (N=37)	Alive (N=11)	Dead (N=26)	p-value
Demographics				
Male (%)	35(94.6)	10(90.9)	25(96.2)	0.519
Age, years	74(63-78)	65(56-71)	77(67-79)	0.016
BSA, m^2	1.90±0.21	1.83±0.18	1.96±0.20	0.083
Laboratory				
Hematocrit (%)	41.7±3.8	43.1±2.5	41.2±4.2	0.175
eGFR, ml/min/m^2	70.6±14.0	73.0±11.1	69.5±15.1	0.499
NTproBNP, pg/mL	196(80–359)	44(17-227)	244(166-387)	0.009
hsTnT, ng/mL	0.051(0.028-0.073)	0.019(0.007-0.049)	0.062(0.039-0.079)	0.002
6MWT, m	331±138	381±163	309±123	0.157
Imaging assessment				
Septal ECV, %	46±11	50±15	58±8	0.036
Global ECV, %	50±7	47±7	52±7	0.204
Perugini				
I (%)	4(10.8)	3(27.3)	1(3.8)	0.106
II (%)	26(70.3)	6(54.5)	20(76.9)	
III (%)	7(18.9)	2(18.2)	5(19.2)	
LV mass, g	294 (229-370)	207 (129-295)	303(261-388)	0.003
LV mass indexed, g/m^2	154 (120-180)	122 (68-179)	160(144-180)	0.028
Max IVS thickness, mm	15.8±3.6	13.6±3.5	16.6±3.3	0.027
LVEF, %	50±15	58±19	47±12	0.043
LAA, cm^2	27.8(22.5–33.1)	23(20.5–30)	28.8(24–34.3)	0.372
RAA, cm^2	23.5(19.5–29.3)	21.0(17.4–22.9)	25.2(22.3–30)	0.032
TAPSE, cm	1.5(1.2–2.3)	1.9(1.6–9)	1.4(1.1–1.7)	0.515
Dec Time, ms	187(165–209.3)	184(166.7–212)	190(160.5–209)	0.747
E/e' average	14.3(12.4–19.2)	11.2 (8.4–14.1)	16(13.6–21.8)	0.071
GLS, %	-14.9±5.9	-10.6±3.1	-16.5±5.9	0.064

ICD, n (%)	4(10.8)	1(9.1)	3(11.5)	1
PPM, n (%)	2(5.4)	1(9.1)	1(3.8)	0.512

BSA stands for body surface area, eGFR for estimated glomerular filtration rate, ECV for extracellular volume, hsTnT for high sensitive troponin T, Max IVS for maximum interventricular septum, LVEF for left ventricular ejection fraction, LAA for left atrium area, RAA for right atrium area, TAPSE for tricuspid annular systolic excursion, Dec for deceleration, and 6MWT for 6 minutes walking test

Table 3: Cox regression analysis for all-cause mortality among ATTR amyloidosis patients.

	Univariate analysis					**Multivariate analysis**				
			95% CI					**95% CI**		
Variable	**HR**	**Wald**	**Inferior**	**Superior**	**p-value**	**HR**	**Wald**	**Inferior**	**Superior**	**p-value**
Age, years	1.042	4.654	1.004	1.083	0.031	1.006	0.051	0.953	1.062	0.822
NTproBNP *	3.98	9.635	1.664	9.519	0.002					
hsTnT *,¥	1.264	7.117	1. 064	1.501	0.008					
ECV, %	1.039	4.143	1.001	1.077	0.042	1.047	4.918	1.005	1.091	0.027
LV mass indexed, g/m^2	1.008	11.885	1.004	1.013	0.001					
Max IVS thickness, mm	1.266	8.798	1.083	1.479	0.003	1.286	10.623	1.105	1.496	0.001
LVEF, %	0.958	8.244	0.930	0.989	0.004	0.976	1.620	0.939	1.013	0.203

ECV stands for extracellular volume, hsTnT for high sensitive troponin T, Max IVS for maximum interventricular septum, LVEF for left ventricular ejection fraction. * Stands for log transformed, ¥ in deciles

FIGURES

Figure legends:

Figure 1:

Title: Increased ECV with higher degrees of cardiac involvement

Caption: Box plots graphic yielding ECV association with higher degrees of cardiac involvement in ATTR (figure 1A) and AL (figure 1B) patients assessed by Perugini and Mayo grade classification, respectively. Note the significantly increased ECV percentages among those with higher degrees in both diseases.

Figure 2:

Title: Whole heart 3D ECV analysis depicts different degrees of cardiac involvement

Caption: Whole heart 3D ECV analysis clearly distinguishes ECV burden throughout the full spectrum, as depicted in different patients with low (figure 2A), intermediate (figure 2B) and high (figure 2C) percentages. Last example corresponds to a patient with ATTR cardiac amyloid involvement highlighting a predominant mid-wall increased ECV pattern.

Figure 3:

Title: The usefulness of whole heart 3D ECV in specific populations

Caption: Whole heart 3D ECV output superimposed in an AHA segmentation allows to distinguish ECV distribution throughout the left ventricle and hypothesize different etiologies affecting the heart with known pattern behavior. In figure 3A it is yielded a patient with ATTR cardiac amyloidosis with a typical apical sparing distribution. Figure 3B represents a patient with a subendocardial increased ECV in the basal to mid lateral wall, showing a myocardial infarct in the LCx territory. Finally, Figure 3C highlights the maintained ability to interpret ECV distribution in a patients with ATTR cardiac amyloidosis with an implanted ICD.

Figure 4.

A.

Title: ECV in patients with amyloid and AS patients

Caption: Myocardial ECV was significantly higher in patients with cardiac amyloidosis (both AL and ATTR cohort) when compared to AS.

B.

Title: Correlation between CMR_{ECV} and CT_{ECV}

Caption: ECV assessed by CT significantly correlated with CMR.

Central Illustration: Title: The advantages of ECV assessment by cardiac CT

Caption: In patients with systemic amyloidosis, ECV by cardiac CT depicts different degrees of cardiac involvement. It is associated with adverse left ventricle remodeling and independently predicts all-cause mortality in ATTR subtype. ECV_{CT} replicates previous findings assessed by CMR but with the important advantage of being faster, cheaper, wide-spread availability, less claustrophobic and not significantly affected by cardiac devices.

Figure 1:

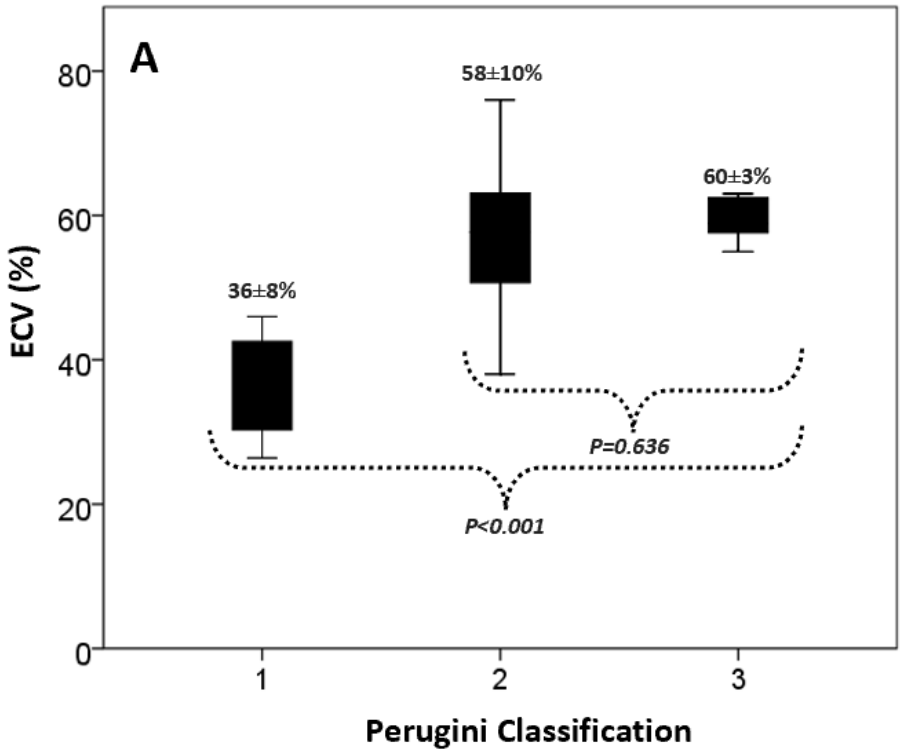
A
80
60
40
20
0
ECV (%)
58±10%
60±3%
36±8%
P=0.636
P<0.001
1
2
3
Perugini Classification

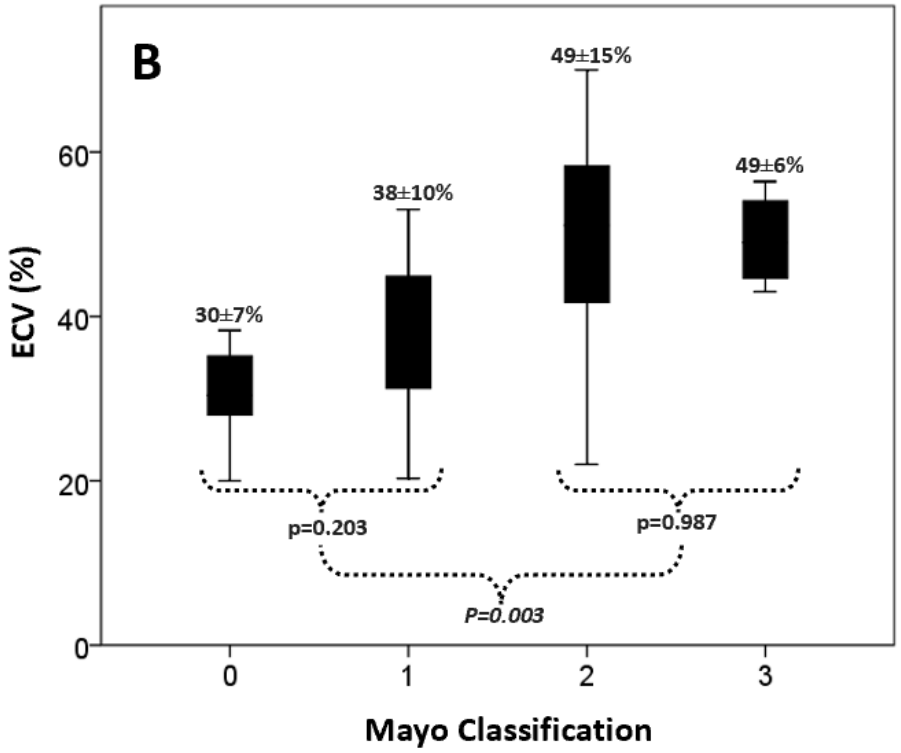
B
60
40
20
0
ECV (%)
49±15%
49±6%
38±10%
30±7%
p=0.203
p=0.987
P=0.003
0
1
2
3
Mayo Classification

Figure 2

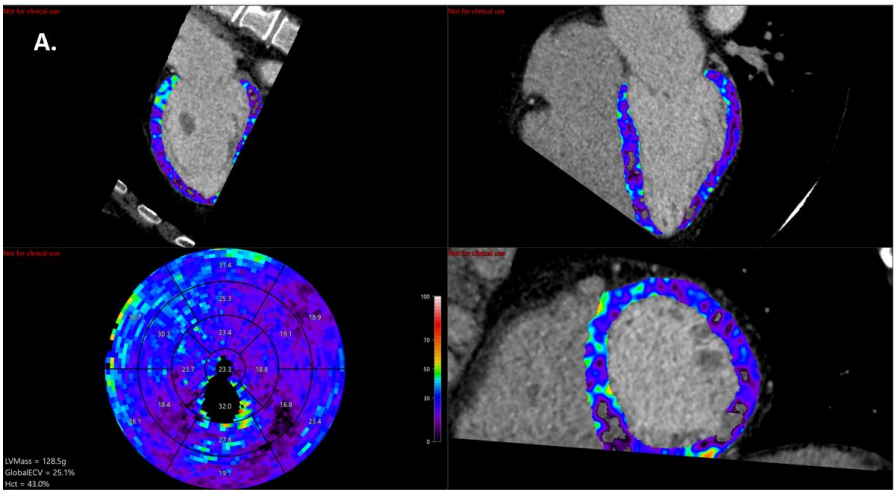
A.
LVMass = 128.5g
GlobalECV = 25.1%
Hct = 43.0%

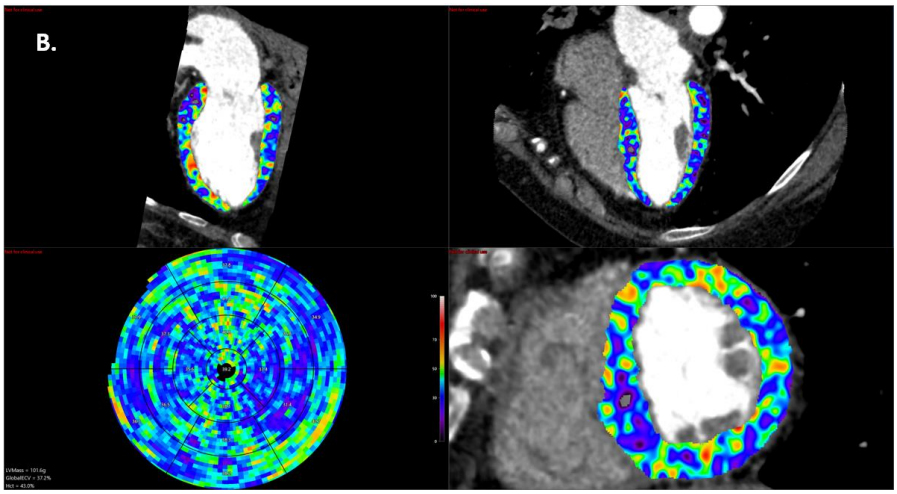
B.

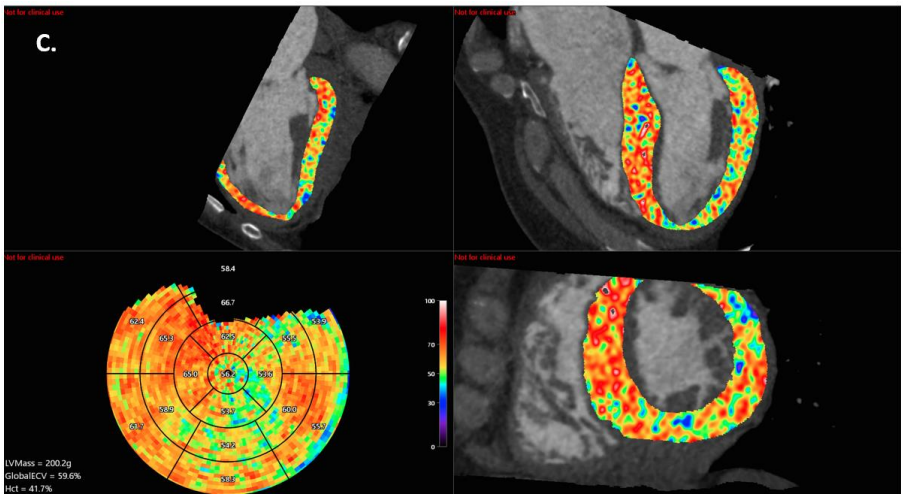
C.
LVMass = 200.2g
GlobalECV = 59.6%
Hct = 41.7%

Figure 3

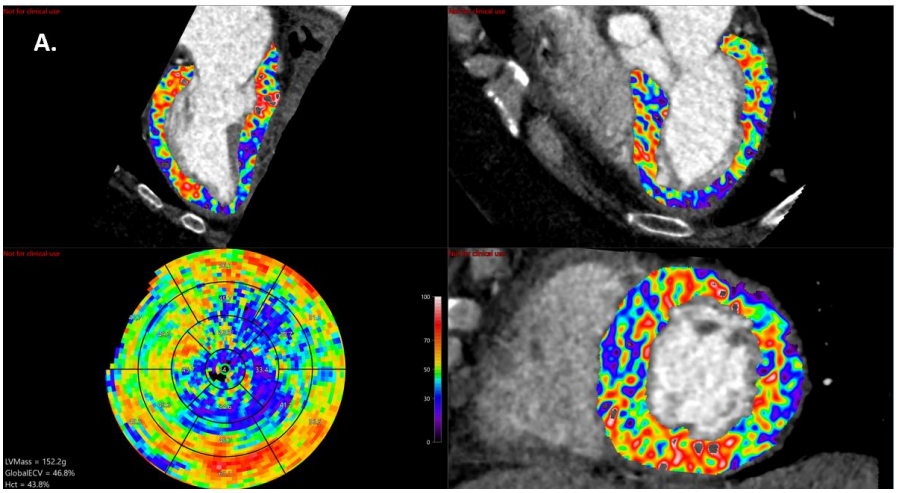
A.
LVMass = 152.2g
GlobalECV = 46.8%
Hct = 43.8%

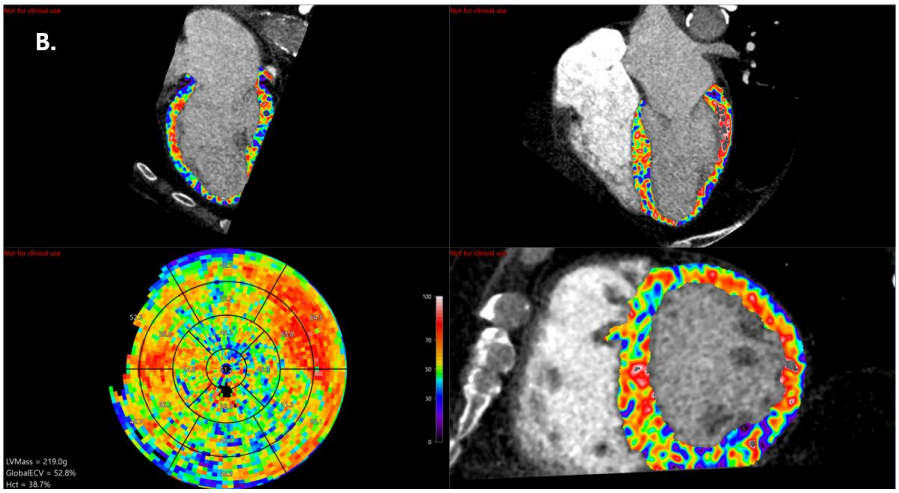
B.
LVMass = 219.0g
GlobalECV = 52.8%
Hct = 38.7%

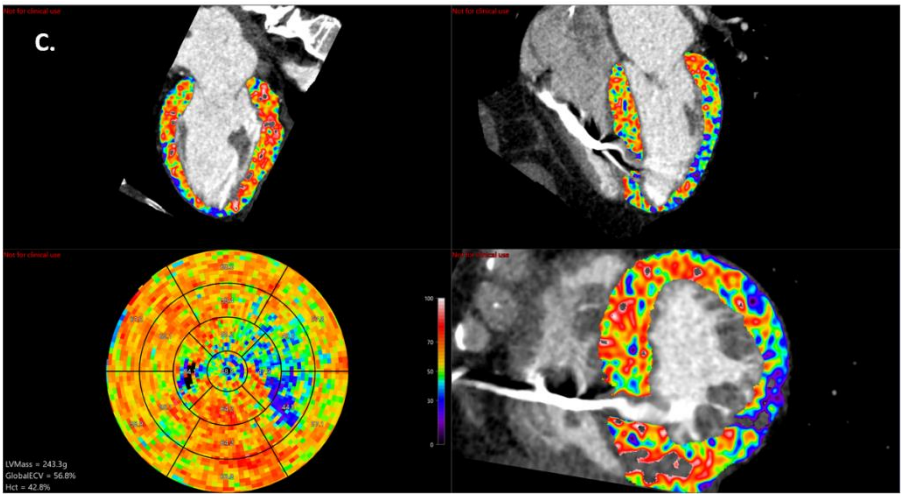
C.
LVMass = 243.3g
GlobalECV = 56.8%
Hct = 42.8%

Figure 4

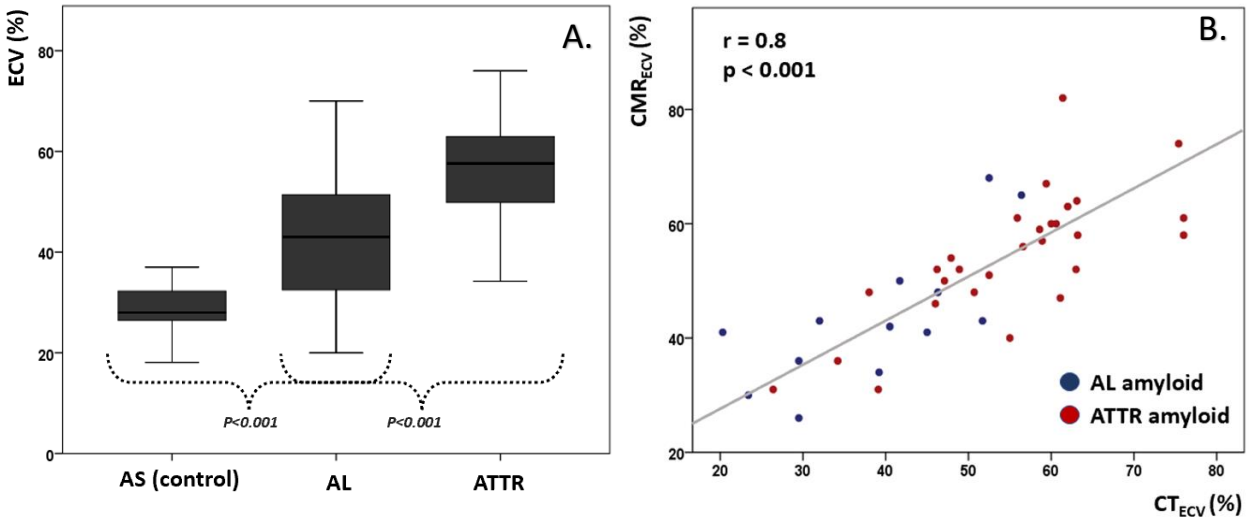
A.
ECV (%)
80
60
40
20
0
P<0.001
P<0.001
AS (control)
AL
ATTR
B.
r = 0.8
p < 0.001
CMR_ECV (%)
80
60
40
20
20
30
40
50
60
70
80
CT_ECV (%)
AL amyloid
ATTR amyloid

1 **Central illustration:**

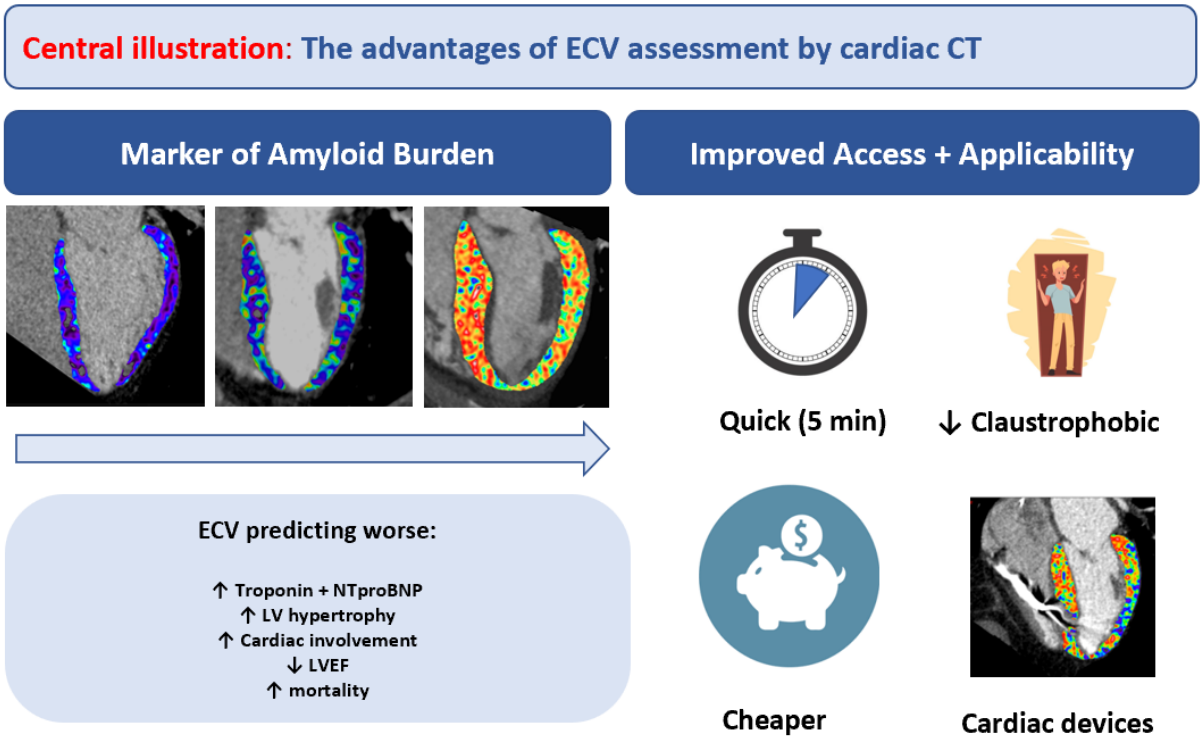

2

3